This is a repository copy of *An alternative simplified model of tensile membrane action of slabs in fire*.

White Rose Research Online URL for this paper:
http://eprints.whiterose.ac.uk/77933/

Version: Published Version

Proceedings Paper:
Burgess, I.W., Dai, X. and Huang, S.S (2013) An alternative simplified model of tensile membrane action of slabs in fire. In: Proceedings of International Conference Application of Structural Fire Engineering. Applications of Structural Fire Engineering conference, 19-20 April 2013, Prague, Czech Republic. CTU Publishing House , Czech Technical University in Prague . ISBN 9788001052044

Reuse
Unless indicated otherwise, fulltext items are protected by copyright with all rights reserved. The copyright exception in section 29 of the Copyright, Designs and Patents Act 1988 allows the making of a single copy solely for the purpose of non-commercial research or private study within the limits of fair dealing. The publisher or other rights-holder may allow further reproduction and re-use of this version - refer to the White Rose Research Online record for this item. Where records identify the publisher as the copyright holder, users can verify any specific terms of use on the publisher's website.

Takedown
If you consider content in White Rose Research Online to be in breach of UK law, please notify us by emailing eprints@whiterose.ac.uk including the URL of the record and the reason for the withdrawal request.

eprints@whiterose.ac.uk
https://eprints.whiterose.ac.uk/

AN ALTERNATIVE SIMPLIFIED MODEL OF TENSILE MEMBRANE ACTION OF SLABS IN FIRE

Ian W. Burgess [a], Xu Dai [a], Shan-Shan Huang [a]

[a] University of Sheffield, Dept. of Civil and Structural Engineering, UK

Introduction

Before 2000, there was only one way of ensuring the fire resistance of steel-framed buildings with composite flooring systems, which was simple but over-conservative. This traditional method considers the composite floor as an array of parallel, simply supported, composite beams, and implies that each of the steel downstand sections which form the tension zone of a composite beam needs to be provided with an insulating cover, in the same way as the non-composite steel columns. This takes no account of the intrinsic fire resistance of the structure due to its continuity.

A simplified design method for composite slabs to resist fire was introduced by Bailey & Moore (2000a, b). This method was based very largely on a calculation of the enhanced load capacity of concrete slabs at high deflections, due to their membrane strength, which had been published by Hayes (1968). The method has since then become widely used in practical fire engineering design, and has recently been published in both the UK (Simms & Bake 2010) and New Zealand (Clifton 2006) as freely-available public-domain design software. Within the EU, the project FRACOF (Vassart & Zhao 2011a, b) has recently extended this simplified method to the Eurocode context, and this project has resulted in a design process which is extremely similar to that in the UK.

In fire conditions, when the temperatures of both unprotected and protected steelwork become extremely high, the mechanism which controls the load resistance of floor systems changes increasingly at high deflections, from the bending strength of the array of composite beams which applies in normal ULS design to tensile membrane action (TMA). In the TMA mechanism the highly deformed concrete slab effectively carries the loading when the strength of the attached downstand steel beam sections has reduced dramatically at high temperatures. TMA can greatly enhance the floor system's load capacity compared with the usual small-deflection load capacity based on the lowest-energy plastic yield-line mechanism. However, the structural mechanics of the Bailey method is not completely transparent; at more than one stage purely empirical assumptions are made. The effects of these assumptions are by no means clear. In this study, a fresh look at Tensile Membrane Action of thin concrete floor slabs at large deflections has been undertaken, with the prime objective of making kinematically consistent assumptions which eliminate the mechanical inconsistencies inherent in the existing methods..

Load and deflection for a kinematically consistent TMA mechanism

A two-way spanning rectangular slab panel of aspect ratio *r*, which is transversely supported along all its four edges, is considered. The slab may either be considered as isolated, in the sense of having no continuity with adjacent panels across these edges, or as continuous in the sense that adjacent panels on all four sides are assumed to be deflecting in the same way as the panel under consideration. The slab is lightly reinforced with a welded mesh, which for the purposes of this paper is considered to be isotropic, and the two layers of bars are assumed to lie at a single mean level within the slab.

The transverse loading intensity on the slab is increased until a plastic yield-line pattern of cracks forms, in the characteristic arrangement shown in Figure 1. The optimum yield-line mechanism, which forms at the lowest possible failure value of the load intensity, is given for either isolated or continuous cases by:

$$n = \frac{1}{2r}\left(-1 + \sqrt{1 + 3r^2}\right) \quad (1)$$

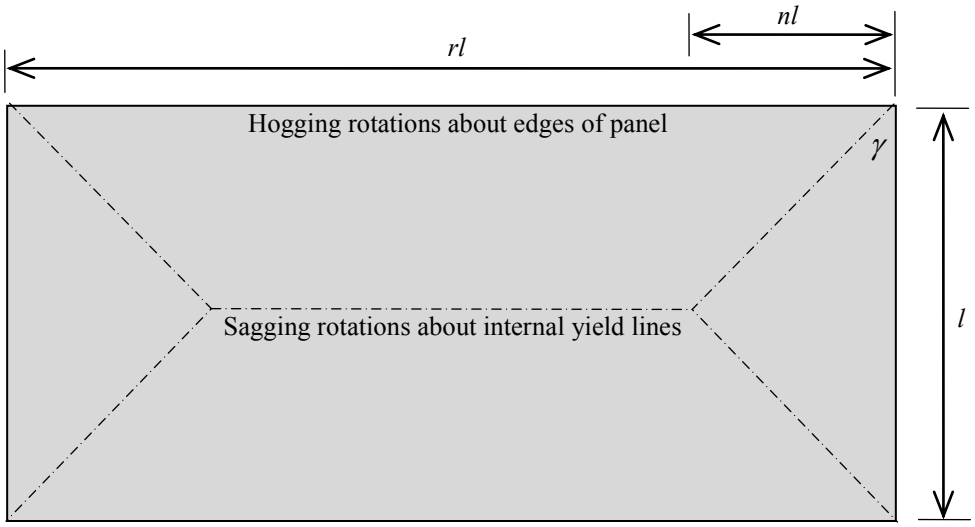

Figure 1: Small-deflection yield-line mechanism

If the load intensity is increased beyond the optimum small-deflection yield-line failure value at which this pattern of folds appears, any further deflection of the flat facets of the slab is assumed to be based on increasing the rotations about the yield lines. The existing simplified methods of calculating enhancement of load capacity due to TMA make use of the consistent observation from tests that a through-depth tensile crack subsequently appears across the shorter mid-span of the slab; in fire this tensile crack provides the possibility of a compartmentation integrity failure. If this crack is assumed to form, then six flat facets (four trapezoidal and two triangular) take part in the subsequent deformation of the slab. It can be seen from Figure 2 that this mechanism causes four different crack types (denoted α, β_1, β_2 and β_3) in different locations

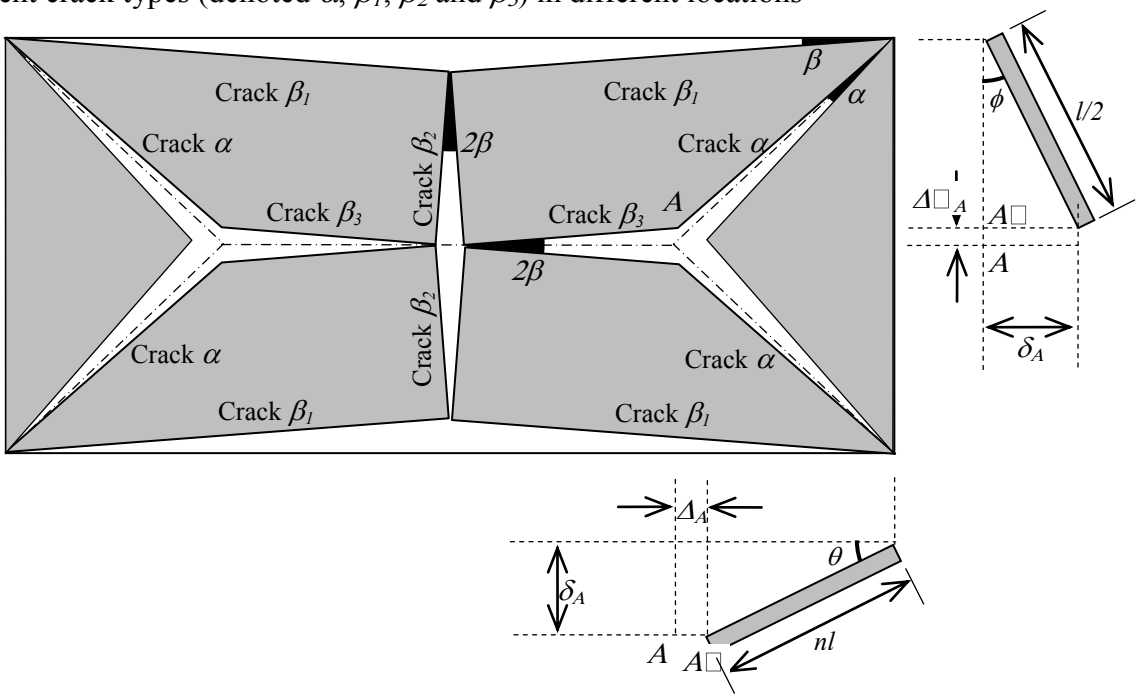

Figure 2: Plan and elevations of the slab facets at high deflection.

It is assumed that internal plastic work is done by stretching the reinforcing bars of the mesh across any relevant cracks; clearly in the case of an isolated slab panel no internal work is done either in cracks β_1 or along the short-span panel edges. Across any crack the mesh bars in the long (x) and short (y) directions stretch independently, and the total internal work therefore consists of the aggregate for all bars which cross cracks of *(the yield force of a bar x the crack crack opening at the level of the bar).* The relationships between the displacement δ_A and the crack opening angles, assuming that the concrete compression zones at the ends of the cracks have negligible length, are:

$$\beta = \frac{1}{2r}\phi^2 \tag{2}$$

$$\alpha = n\theta^2 cos^2\gamma + \phi^2\left[\left(\frac{1}{2} - \frac{n}{r}\right) sin\gamma . cos\gamma - \frac{1}{2r}cos^2\gamma\right] \tag{3}$$

in which

$$\theta = \frac{\delta_A}{nl} \qquad \phi = \frac{2\delta_A}{l} \qquad \gamma = tan^{-1}(2n) \tag{4}$$

The crack opening in either the *x* or *y* directions at a particular rebar location is a function of the crack opening angle and of the rotation angle about the perpendicular axis between the slab facets which meet at the crack. The principle is illustrated in Figure 3.

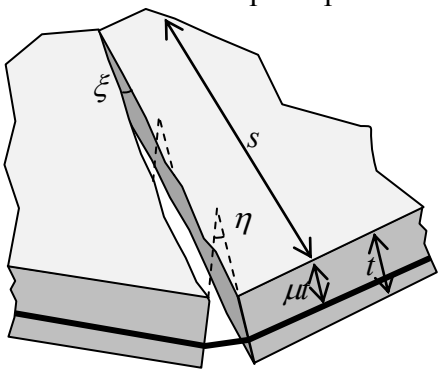

Figure 3: Crack opening at rebar level.

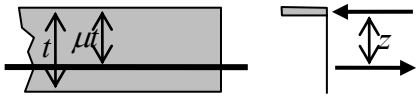

Figure 4: Assumed reduced effective depth.

If the crack pivots about its top edge then the rebar extension is *(ξs + ημt)*. However, a finite area of concrete at the top edge of the crack is actually needed to balance the tensile force across the crack. Although it may eventually be necessary to represent the exact size and shape of the compression area at the closed end of a crack, the assumption of balanced stress blocks, shown in Figure 4, which is made in the existing simplified methods, is also used here to slightly reduce the lever arm from $z = \mu t$ to

$$z = \mu t - \frac{1}{2}\left(\frac{f_y A_r}{f_c}\right) = \mu t - \frac{1}{2}\left(\frac{F_p}{f_c}\right) \tag{5}$$

in which A_r is the reinforcement area per unit slab width, and F_p is the yielded bar force per unit width of slab. It can be assumed that the reinforcement bars have a fracture ductility strain of ε_u, and that a bar anchors positively into the concrete where transverse bars are welded to it. The fracture strain is assumed to act on the transverse bar spacing to define a fracture crack width at the reinforcement level, with no diminution due to bond between the concrete and rebar. As a crack opens, the wide end will reach a width at which the bars begin to fracture, and with further opening the length of crack over which bars are fractured will increase. The components of the internal plastic work for the sagging yield lines are then expressed in terms of the dimensionless quantities:

$$\bar{t} = t/l \qquad \nu = \frac{\Delta_{lim}}{l} = \frac{d_{sp}}{l}\varepsilon_u \tag{6}$$

in which d_{sp} is the inter-bar spacing in both directions and Δ_{Lim} is the crack width at which rebar fracture occurs.

For each yield line the plastic internal energy due to the *x*- and *y*-direction rebars can be calculated individually, over the length of the yield line (X or Y) for which the corresponding rebars are unfractured. Dimensionless versions of these unfractured lengths are denoted $\bar{X} = X/l$ and $\bar{Y} = Y/l$.

The components of the internal plastic energy are then shown in Table 1. These are aggregated at each deflection step to form the total internal energy. Clearly, for an isolated slab, the components generated along the long and short slab edges are zero.

Table 1: Internal plastic energy components of slab at large deflections.

Crack	Rebar direction	Maximum rebar length/*l*	Intact rebar length/*l* if bars fractured	Internal plastic energy	Factor for whole slab
α	*x*	$\bar{Y} = 0.5$	$\bar{Y} = \frac{(\nu - \theta\mu\bar{t})}{\alpha}$	$W_{int,\alpha x} = F_p l^2 \bar{Y}\left(\frac{\alpha}{2}\bar{Y} + \theta\mu\bar{t}\right)$	4
	y	$\bar{X} = n$	$\bar{X} = \frac{(\nu - \phi\mu\bar{t})}{\alpha}$	$W_{int,\alpha y} = F_p l^2 \bar{X}\left(\frac{\alpha}{2}\bar{X} + \phi\mu\bar{t}\right)$	4
β_1	*y*	$\bar{X} = \frac{r}{2}$	$\bar{X} = \frac{(\frac{\nu}{2} - \phi(1-\mu)\bar{t})}{\beta}$	$W_{int,\beta 1} = F_p l^2 \bar{X}\left(\frac{\beta}{2}\bar{X} + \phi(1-\mu)\bar{t}\right)$	4c*
β_2	*x*	$\bar{Y} = 0.5$	$\bar{Y} = \frac{\nu}{2\beta}$	$W_{int,\beta 2} = F_p l^2 \bar{Y}(\beta\bar{Y})$	2
β_3	*y*	$\bar{X} = \left(\frac{r}{2} - n\right)$	$\bar{X} = \frac{(\nu - 2\phi\mu\bar{t})}{2\beta}$	$W_{int,\beta 3} = F_p l^2 \bar{X}\left(\frac{\alpha}{2}\bar{X} + \phi\mu\bar{t}\right)$	2
Short edge	*x*	$\bar{Y} = 1$	0	$W_{int,l} = F_p l^2 \bar{Y}(\theta(1-\mu)\bar{t})$	2c*

* *c=0 for isolated slab, c=1 for continuous slab.*

The aggregate internal energy is then

$$W_{int} = W_{int,\alpha x} + W_{int,\alpha y} + \sum_{i=1}^{3} W_{int,\beta i} + W_{int,l} \quad (7)$$

The external work (or loss of potential energy) of the uniform transverse loading, of intensity p, is expressed in the same way as for small deflections:

$$W_{ext} = p l^2 \delta_A \left(\frac{r}{2} - \frac{n}{3}\right) \quad (8)$$

Since rigid-perfectly plastic behaviour is being assumed for the reinforcing mesh,

$$W_{ext} = W_{int} \quad (9)$$

Thus the load capacity of the slab, at any deflection δ_A, is therefore:

$$p = W_{int} \Big/ \left[l^2 \delta_A \left(\frac{r}{2} - \frac{n}{3}\right)\right] \quad (10)$$

Comparisons with the conventional simplified methods

Figure 5 shows an example comparison between the load capacity enhancements given by the conventional methods and the new proposal. The example is for a 9m x 6m isolated slab 120mm thick, with A142 mesh (6mm bars at 200mm spacing in both directions) at the mid-depth (60mm from the top) of the slab. The steel grade is S500 and the concrete C30. In this case the fracture ductility of the reinforcing steel has been assumed to be 5%. In presenting the limiting deflection of the slab in the context of the conventional methods the component of that deflection which is derived from the assumed thermal bowing of the slab has been ignored, because the TMA is being considered independent of any temperature effects. It can be seen that the enhancement of capacity due to deflection differs between the methods; the new approach shows a lower rate of enhancement for this particular slab case. The new approach is capable of showing where reinforcement fracture begins and is completed for each yield line.

In this particular case the limiting deflection given in the Bailey/BRE or FRACOF methods occurs at roughly the same deflection as the peak load capacity which is caused by the start of rebar fracture in the longitudinal yield line β_3.

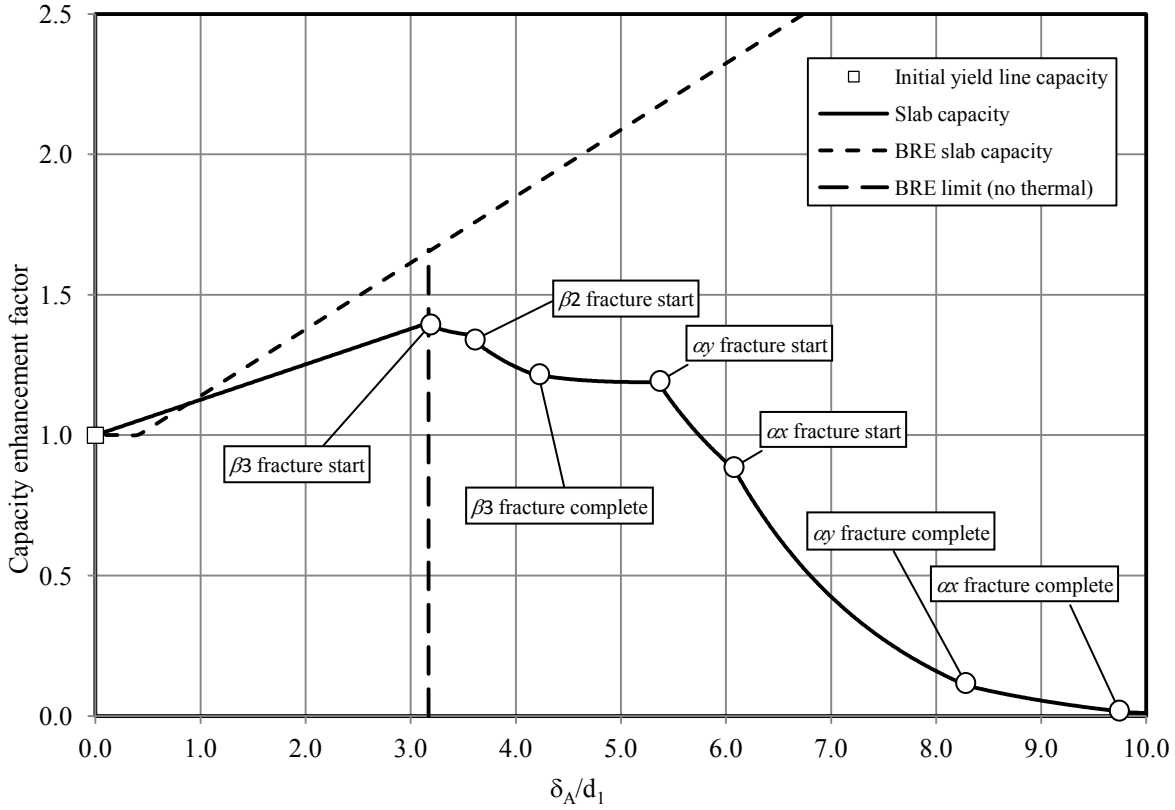

Figure 6: Enhancement of yield-line capacity of a 9m x 6m slab according to the BRE and current approaches.

However it is seen from Figure 7, which considers different steel ductilities, that there is no inherent connection involved.

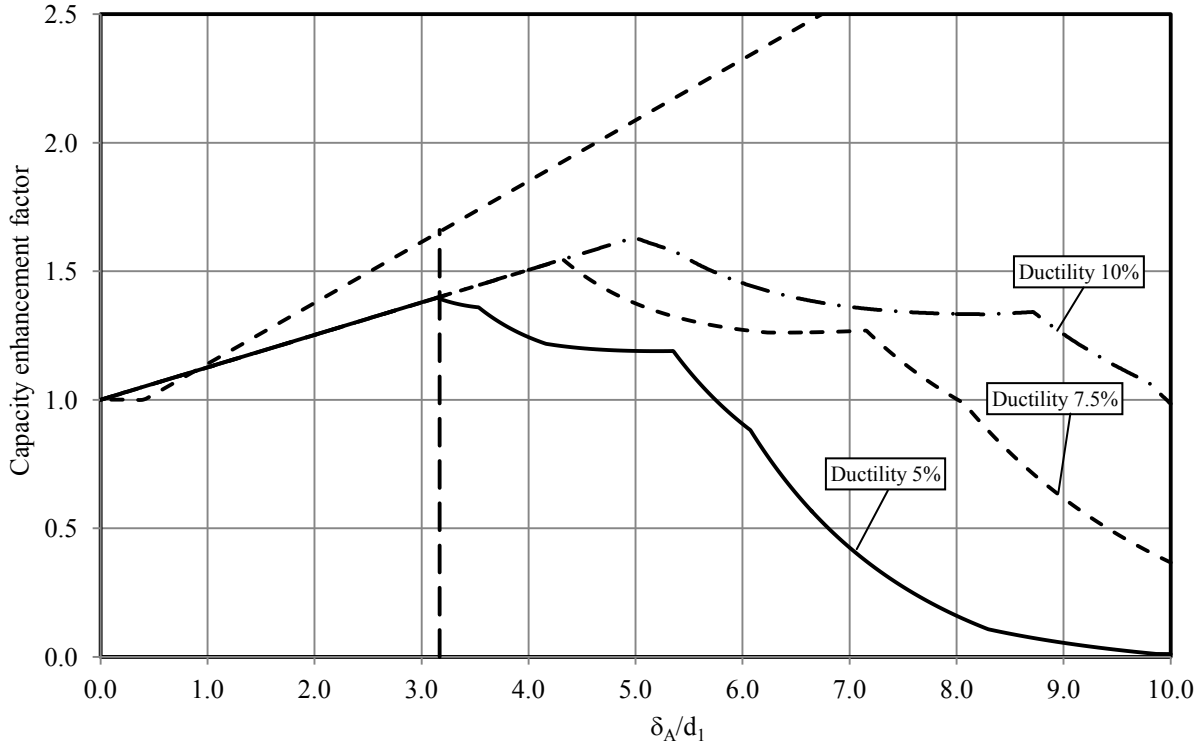

Figure 7: Comparison between BRE method and the new approach for different rebar fracture ductilities.

In order to gauge how this approach correlates to the existing methods for slabs of different aspect ratio, the predicted enhancements of capacity for three slabs, 6m x 6m, 6m x 9m and 6m x 12m, reinforced as in the previous cases, are shown in Figure 8. Clearly the actual yield-line capacities of the three cases are different, but since the enhancement factors are plotted, all of the curves begin at

1.0 enhancement at zero deflection. It can be seen that the gradients of the enhancements with intact reinforcement for any aspect ratio differ between the two approaches; the discrepancy appears highest for the square panel, for which the ratio of the gradients is 0.45. For the slab of aspect ratio 2.0 the enhancement the enhancement gradients are almost identical.

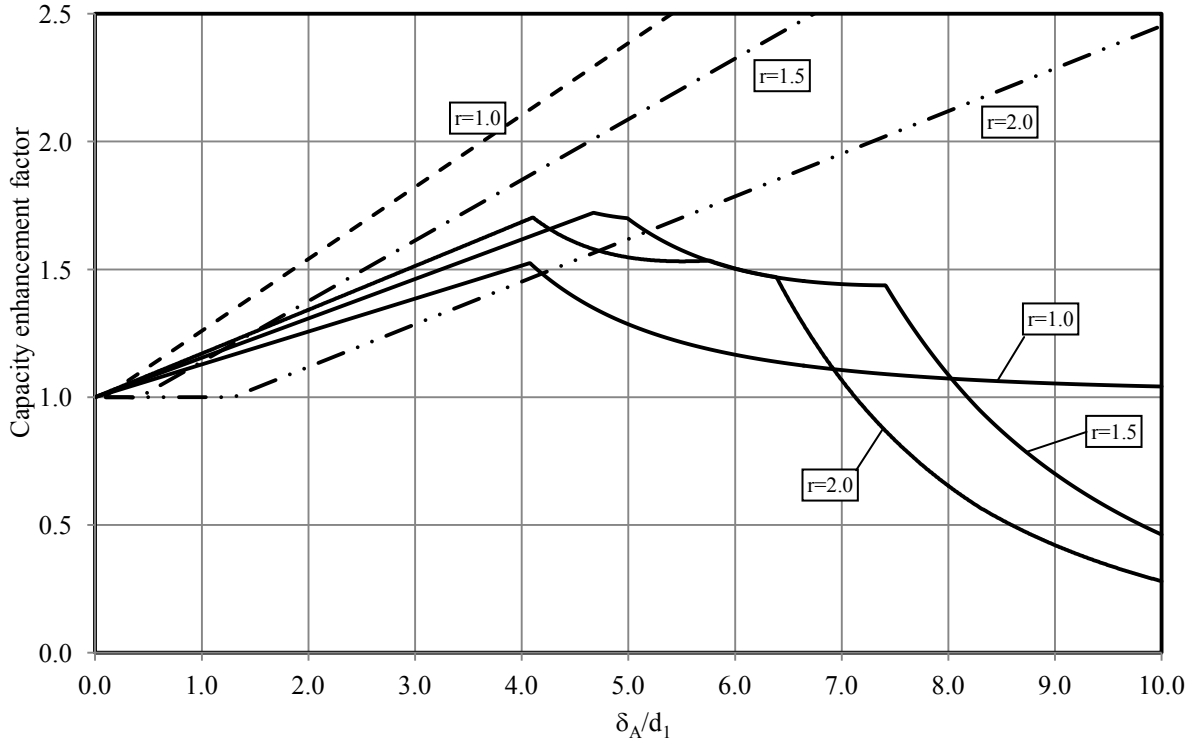

Figure 8: Comparison between BRE enhancements and the new approach for different slab aspect ratios.

Discussion

The method developed here appears to have the advantage over the preceding approaches that it is clearly based on a kinematically admissible deflection model, and involves no arbitrary aggregation of "enhancements" from four different sources. The approach is easily capable of being extended to account for continuity, concrete crushing failure, orthotropic mesh and a rebar-concrete bond model. It can also examine different kinematically admissible deflection mechanisms without any change to its basic methodology; allowing lower-bound to be identified.

References

Bailey, C.G. and Moore, D.B. (2000a), "The structural behaviour of steel frames with composite floor slabs subject to fire - Part 1 Theory", *The Structural Engineer* , **78** (11), pp 19-27.

Bailey, C.G. and Moore, D.B. (2000b), "The structural behaviour of steel frames with composite floor slabs subject to fire - Part2: Design", *The Structural Engineer*, 78(11), pp28-33.

Hayes, B. (1968), "Allowing for membrane action in the plastic analysis of rectangular reinforced concrete slabs", *Magazine of Concrete Research*, **20** (65), pp205-212.

Simms, W.I. and Bake, S. (2010), "TSLAB V3.0 User Guidance and Engineering Update", SCI publication P390.

Clifton, C. (2006), "Design of composite steel floor systems for severe fires", HERA publication, Manukau City, New Zealand.

Vassart, O. and Zhao, B. (2011a), "FRACOF : Fire resistance assessment of partially protected composite floors: Engineering Background", Arcelor/Mittal & CTICM.

Vassart, O. and Zhao, B. (2011b), "FRACOF : Fire resistance assessment of partially protected composite floors: Design guide", Arcelor/Mittal & CTICM.